JOURNAL OF GEOPHYSICAL RESEARCH, VOL. 101, NO. D16, PAGES 21,391–21,402, SEPTEMBER 27, 1996

Numerical simulations of stratocumulus processing of cloud condensation nuclei through collision-coalescence

Graham Feingold
Cooperative Institute for Research in the Atmosphere, NOAA, Colorado State University, Fort Collins

Sonia M. Kreidenweis, Bjorn Stevens, and W. R. Cotton
Department of Atmospheric Science, Colorado State University, Fort Collins

Abstract. The role of drop collision-coalescence as a means of reducing drop number concentrations, and hence cloud condensation nucleus (CCN) concentrations as these are cycled in the stratocumulus-capped marine boundary layer, is investigated. We focus on the impact of this process on the mass-mean size of CCN in the absence of wet deposition, and compare this mechanism with size changes resulting from mass addition through aqueous chemistry. The modeling framework is a two-dimensional eddy-resolving model that includes explicit treatment of aerosol and drop spectra, as well as the solute transfer between drop size bins. The microphysical processes considered are droplet activation, condensation/evaporation, collision-coalescence, sedimentation and regeneration of particles following complete evaporation. It is shown that for a case exhibiting negligible wet deposition, collision-coalescence can significantly reduce drop concentrations (22% h^{-1}) resulting in a measurable increase in particle mass-mean radius of about 7% h^{-1}. In order to extend the validity of these results, trajectory analyses of parcel in-cloud residence times have been used together with box model calculations of collision-coalescence to explore the parameters affecting processing through collision-coalescence. This trajectory information is also used to deduce the extent of in-cloud conversion of SO_2 to sulfate. Comparisons show that the two mechanisms may produce comparable rates of increase in the mean particle size under certain conditions. Results for remote marine conditions suggest that aqueous phase chemistry may have a greater impact at lower cloud liquid-water contents, whereas collision-coalescence may dominate at higher liquid-water contents, or for broader drop spectra.

1. Introduction

Studies of the marine boundary layer show increasing evidence that the atmospheric aerosol, and particularly those particles that serve as cloud condensation nuclei (CCN), not only impact clouds [e.g., *Twomey*, 1974, 1977; *Albrecht*, 1989], but that clouds in turn exert a measurable influence on the abundance and characteristics of CCN [*Hegg and Hobbs*, 1982; *Baker and Charlson*, 1990; *Bower and Choularton*, 1993]. The impact of clouds on CCN can take place via different mechanisms. First, there is evidence for the nucleation of high concentrations of new sulfate particles just above cloud top [*Hegg et al.*, 1990], apparently produced by homogeneous, heteromolecular nucleation in regions of high relative humidity. This process replenishes aerosol number concentrations, and may ultimately serve as a source of CCN if these particles grow to appropriate sizes. Second, various aqueous phase chemical processes deposit mass in droplets and enhance the amount of soluble material [*Hegg and Hobbs*, 1982; *Chameides*, 1984; *Bower and Choularton*, 1993]. On complete evaporation, each droplet produces a single particle [*Mitra et al.*, 1992]. Thus, aqueous chemistry enhances particle mass concentrations without impacting particle number concentrations, with the result that CCN are on average larger and more easily activated at ambient supersaturations.

Another pathway for cloud processing of aerosol, and the one investigated here, is via drop collision-coalescence [e.g., *Hudson*, 1993; *Garrett and Hobbs*, 1995]. Consider a cloud whose drops undergo collision-coalescence in addition to condensation/evaporation cycles. If collision-coalescence is able to significantly deplete drop concentration, then aerosol number concentrations, and specifically the number concentration of the CCN fraction, will be reduced following evaporation of the cloud. The depletion in CCN concentration will depend upon the depletion in drop number, and upon the percentage number of CCN activated from the total CCN population. With no accompanying change in CCN mass (i.e., in the absence of aqueous chemistry), this depletion in particle number will result in a spectrum with increased mass-mean radius.

The three cloud-processing mechanisms cited above may act to varying degrees in all clouds, and no attempt is made to study all of these processes. Rather, it is our intent to examine the collision-coalescence processing effect for some selected cases, and attempt to assess its magnitude relative to that of aqueous chemistry. The cloud-topped marine boundary layer (MBL) is the focus of this study for several reasons: its importance in the global radiation budget [e.g., *Nakajima and King*,

Copyright 1996 by the American Geophysical Union.

Paper number 96JD01552.
0148-0227/96/96JD-01552$09.00

1990]; the proposed sensitivity of the cloud properties to changes in CCN concentrations [e.g., *Twomey*, 1977]; and the generally low CCN concentrations present in this system, which magnify the impacts of cloud processes on the aerosol [e.g., *Albrecht*, 1989]. Our approach is to develop and apply a numerical model that can be used to develop estimates of the magnitude of the effects of collision-coalescence, considered separately from other processes and for specific, limited timescales. Then, the magnitude of the effects of aqueous chemistry on similar timescales is examined.

In order to address these issues in a numerical model, a framework that predicts CCN and drop spectra in an explicit sense (i.e., bin-resolved spectra), and also calculates properties of the CCN in solution is required. This is true for studies of both aqueous chemistry processing and collision-coalescence processing. A number of previous studies have included some level of knowledge of drop solute. Pioneering work by *Flossmann et al.* [1985] calculated bulk properties of solute (e.g., total mass), whereas more recent work by *Trautmann* [1993] and *Chen and Lamb* [1994] solves for a two-dimensional drop size distribution $n(x, a)$, where x represents drop mass and a represents aerosol mass. These techniques provide a more complete description of CCN-drop interactions than the bulk approach. Nevertheless, they are computationally extremely expensive and to date have only been included in one-dimensional models, or kinematic models with prescribed flow.

In this work an attempt is made to provide a balance between resolution of CCN spectra, drop spectra, and cloud processing of CCN on the one hand, and the dynamics of a stratocumulus-capped boundary layer on the other. It is noted that the vertical velocity field w is critically important in a number of respects. First, it is responsible for generating local supersaturation and the activation of droplets, and second, as shown by *Feingold et al.* [1996], it plays an important role in drizzle-drop formation by determining in-cloud residence times. The issue of in-cloud residence time is central in a number of regards. It determines the time available for aqueous chemistry before a parcel leaves the cloud; it determines the time available for collision-coalescence to deplete drop number (and by induction, CCN concentration); and it determines whether precipitation will form. Precipitation (although not the focus of this work) is in turn important, both as a means of removing CCN number and mass, but also as a way to modify the thermodynamic structure of the boundary layer. Indeed, drizzle has been implicated as a possible means for decoupling the boundary layer and breaking up stratocumulus decks [*Nicholls*, 1984; *Paluch and Lenschow*, 1991]. The nature of this interaction between microphysics and dynamics in stratocumulus environments is such that both processes must receive due attention.

Simple dynamical frameworks are unable to predict probability distribution functions (PDFs) of w or in-cloud residence time very well, and even two-dimensional models produce PDFs that differ from full three-dimensional models [e.g., *Stevens et al.*, 1996]. *Kogan et al.* [1994] recognized this limitation and examined the regeneration of CCN from cloud drops using various ad hoc schemes within a three-dimensional large eddy simulation (LES) framework. However, that study did not include solute transfer between drop bins, which is needed to evaluate the effects of collision-coalescence on the CCN spectrum.

With these issues in mind, for the purposes of the study presented here, a two-dimensional dynamical framework for the MBL, and bulk treatment of solute within each bin of an explicit drop microphysics scheme has been chosen. Details of this model formulation are furnished in section 2. This model is used to examine the spatial distribution of CCN during the development and evolution of the stratocumulus-topped MBL, and the spatial variation of changes in the CCN spectrum attributable to collision-coalescence processing in the absence of wet deposition. The structure of the MBL produced in our model is also examined to ensure that it is physically reasonable, supporting its use for the study of aerosol processing. It should be mentioned that, although three-dimensional numerical experiments coupled to this microphysical treatment are feasible on larger-scale computers, the number and scope of such simulations would be limited. We instead have opted to present results from several two-dimensional studies designed to test the sensitivity of the MBL development to details of the microphysical scheme. Using these results, it is shown in section 4 that, with appropriate averaging techniques, the processing of aerosol can be investigated using a parcel-model framework, further increasing the parameter space that can be explored. In addition, use is made of previous three-dimensional MBL studies to perform this averaging, mitigating the drawbacks of basing processing estimates only on the two-dimensional simulations. Section 4 also discusses the significance of these results and compares them to aerosol processing due to aqueous chemistry.

2. Model Description

The model used in this study is the LES version of the Regional Atmospheric Modeling System (RAMS) model developed at Colorado State University [*Pielke et al.*, 1992], that calculates droplet growth explicitly following the moment-conserving techniques of *Tzivion et al.* [1987, 1989]. It is used in its two-dimensional form, and as such is more correctly termed an eddy-resolving model (ERM), rather than an LES model. It has been applied to stratocumulus studies in a number of works [*Feingold et al.*, 1994, 1996; *Stevens et al.*, 1996] that have investigated various aspects of CCN-cloud interactions and drizzle formation. A critical analysis of the model and the LES technique can be found by *Stevens et al.* [1996].

The model is nonhydrostatic and compressible. Predictive equations are solved for two velocity components (u, w), liquid-water potential temperature, θ_l, perturbation Exner function π, and total water-mixing ratio r_t. An important feature of the explicit microphysical routines is that they solve for both number and mass concentrations of drops in each of the 25 drop bins. The drop bins are defined through the mass-doubling formula

$$x_{k+1} = 2x_k, \tag{1}$$

spanning the radius space (1.5625 μm; 500 μm). The processes of drop condensation/evaporation, stochastic collection and sedimentation are all taken into account. In addition, prognostic equations are solved for 14 size bins of CCN and again both number and mass concentration in each bin are conserved. CCN bins are described by

$$a_{k+1} = 4a_k \tag{2}$$

and span the radius space (0.0056 μm; 7.3 μm). The aerosol is assumed to be chemically homogeneous, with the thermodynamic properties of sodium chloride; thus, the term "CCN" is

used interchangeably with "aerosol" in this discussion. Droplet activation is based on the assumed aerosol composition and on the cloud supersaturation, calculated as in work by *Stevens et al.* [1996]. This activation scheme differs from those previously used by *Feingold et al.* [1994, 1996] and *Stevens et al.* [1996] and is due to *Richardson et al.* [1995]. In order to activate part of a CCN bin, it uses the linear bin distribution function proposed by *Chen and Lamb* [1994]. Mapping of newly activated CCN to drop bins is performed assuming a (variable) subequilibrium size [*Mordy*, 1959]. The degree to which these particle sizes are subequilibrium is directly proportional to the size of the CCN. Those activated CCN that do not achieve the size of the lowest drop bin are placed at the lower end of the first drop bin.

2.1. Modifications for This Study

The major modification in this study is the inclusion of algorithms that keep track of solute within the drops following the activation of CCN [e.g., *Flossmann et al.*, 1985]. However, in contrast to that work, which solved for the value of drop spectra at discrete points, the current work employs a moment-conserving approach whereby moments of the bin distribution function are predicted. In addition to droplet mass and number in a bin (M_k and N_k, respectively), we also predict on the solute concentration in a bin, S_k. This brings the total number of equations for drop and CCN related scalars to 103; 25 equations for each of N_k, M_k, and S_k, and 14 equations for both the number and mass of aerosol in a bin.

Solute is transferred from one bin to another via the processes of condensation/evaporation and stochastic collection. The former are solved on an Eulerian grid (described more fully below), using the technique of *Tzivion et al.* [1989], with solute moving at the same rate as the droplet growth rate. In the case of collection, it is noted that the *Tzivion et al.* [1987] algorithm is written in a manner that permits the identification of individual interactions between bins. Thus, solute is easily and efficiently moved between bins at a rate determined by the collection kernel for the drops. Each of these algorithms conserves solute mass absolutely. The parent algorithms for drop interactions conserve total number in the case of condensation, and total mass in the case of collection.

2.2. Regeneration

The process of regeneration of particles following complete evaporation follows the principle that one particle is regenerated for every drop evaporated [*Mitra et al.*, 1992] and is thus facilitated by knowledge of N_k, which represents when summed over the spectrum, the potential number of CCN that can be regenerated. The treatment of regeneration of CCN following the evaporation of droplets is central to the current investigation, and will be discussed here in some detail. The most appropriate way to study regeneration is through the use of a Lagrangian (moving) mass-grid; in this scheme, drops are identified by their dry particle size, that is, by the size of the particle on which they formed. Drops are then allowed to grow or evaporate depending on the ambient water saturation ratio, and the characteristics of the CCN particle within the drop are fully retained. Unfortunately, the stochastic collection equation is not amenable to solution on a Lagrangian grid. Each collision-coalescence event between drops would generate a new particle size and a rapid proliferation of discrete points to be followed. Moving mass grids are also not suitable for use in Eulerian (fixed) spatial grids.

Since the current study focuses on the collision-coalescence mechanism, an Eulerian framework (both in mass and physical space) has been selected. On an Eulerian mass grid, the size distribution is often defined according to integral quantities within a drop bin bounded by mass limits $(x_k; x_{k+1})$. The fact that bins have a discrete width necessarily implies that size information is limited. Moreover, since bins are normally designed to become broader with increasing mass, as seen in (1), some resolution is lost as drops and solute are moved into larger bins. This problem limits the information that can be retrieved during droplet evaporation and regeneration. As the current microphysical framework has been designed to conserve CCN mass and number, at a minimum, information on the mass-mean radius of CCN can be retrieved. However, before drawing conclusions regarding detailed structure in the processed CCN spectrum, one must first establish that these features are not a numerical artifact of the regeneration scheme.

A number of regeneration schemes have been tested. The first distributes the regenerated mass and number of particles according to a lognormal distribution with fixed geometric standard deviation σ. This scheme will henceforth be referred to as R_{logn}. An alternative method involves the calculation of the breadth parameter [*Turco et al.*, 1979; *Ackerman et al.*, 1995], rather than applying a fixed value; this requires prognostic equations for an additional moment in the 14 aerosol bins, as well as 25 prognostic equations for tracking the property of the solute within the drop bins. We have also implemented such a scheme (R_{logn3}), but selected as the additional moment the particle surface area (the second moment with respect to radius) rather than radar reflectivity (the sixth moment with respect to radius), since the ratio of particle mass to surface area provides direct calculation of the radiatively important particle effective radius.

The third scheme tested, which has been adopted for the majority of the simulations presented in this study, regenerates particles in a manner commensurate with the degree of depletion of a given CCN bin [*Cotton et al.*, 1993]. Since large CCN are more readily activated, the bins representing the larger CCN have a higher probability of receiving regenerated particles than lower bins. Mathematically, this can be written as follows. A function $\phi_k(t)$ is defined such that

$$\phi_k(t) = \frac{\bar{N}_k^a(0) - \bar{N}_k^a(t)}{\bar{N}_k^a(0)}, \tag{3}$$

where k represents a CCN bin, and $\bar{N}_k^a(0)$, and $\bar{N}_k^a(t)$ represent the domain averaged number of CCN in bin k at times 0 and t, respectively. Then, the number of particles regenerated to bin k (R_k) is

$$R_k(t) = N_r(t) \frac{\phi_k(t)}{\sum_{k=1}^{14} \phi_k(t)}, \tag{4}$$

and $N_r(t)$ is the total number of particles regenerated. Regeneration of particle mass uses (4) and the assumption that particle mass resides at the bin center. This scheme will henceforth be referred to as R_{act}.

2.3. Omissions

In the current study, impaction scavenging of CCN is neglected since it is of secondary importance [*Flossmann et al.*, 1985]. Particle coagulation is neglected. Homogeneous nucle-

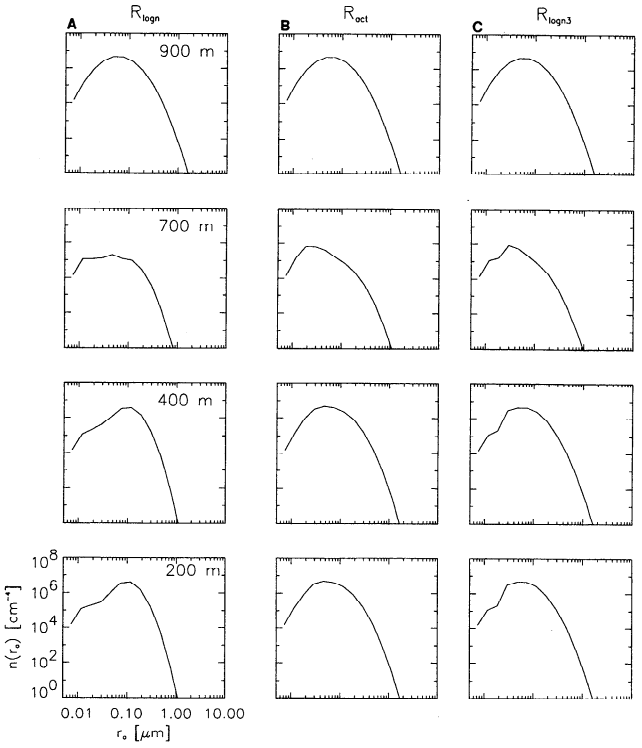

Figure 1. Layer averaged cloud condensation nucleus (CCN) spectra at select heights for the case of no collision-coalescence after 120 min. Regeneration schemes used are (a) the R_{logn} scheme (lognormal, fixed σ); (b) the R_{act} scheme based on activation history; (c) a lognormal scheme with variable σ based on a three-moment representation of solute.

ation of new particles from the gas phase is also ignored. Inclusion of such processes would be of interest in a more comprehensive study, but would detract from our examination of the roles of the processes of primary interest here. Thus, in these experiments, the only manner in which CCN spectra can be modified is through what will be termed "physical processing" or "collision-coalescence processing."

2.4. Initial Conditions

The model is initiated with the July 7, 1987, sounding from the First International Satellite Cloud Climatology Project (ISCCP) Regional Experiment (FIRE) held off the coast of California (see the stratocumulus sounding presented by *Betts and Boers* [1990]). Boundary conditions include a fixed sea surface temperature, cyclic boundary conditions in the horizontal, and a rigid lid at the top of the model. Longwave radiation is parameterized following *Chen and Cotton* [1983]. Shortwave radiation is not simulated. The model is initialized with a random perturbation of ±0.1 K at the lowest model level. The domain size is 3000 m in the horizontal and about 1400 m in the vertical, with a Δz of 25 m and a Δx of 50 m. A time step of 2 s is used for all but the acoustic terms. This sounding has been chosen because it produces little, or no precipitation for CCN concentrations on the order of 50 cm^{-3} or higher, and thus eliminates the effect of precipitation removal on the CCN spectrum. Note that the simulations to be presented are not intended to be case studies of this event, but rather to provide a physically plausible framework for investigating the processes under discussion.

The two-dimensional simulations take on the order of 24 hours CPU on a 60-MHz processor workstation. Although many of these simulations have been performed, only a few representative results will be presented.

3. Results of MBL Simulation

3.1. Regeneration Experiments Excluding Collision-Coalescence

As discussed above, the ability to discern processing of the CCN spectrum may be limited by the manner in which particles are regenerated. The first set of experiments considers a cloud in which the only cloud processes simulated are activation, condensation, and evaporation. In this case, there should be no processing of CCN spectra, so that the ideal scheme would exactly regenerate the input spectra. The runs shown here initialize the CCN fields according to a lognormal distribution with total number, N = 50 cm^{-3}, median radius r_g = 0.08 μm, and geometric standard deviation σ of 1.8 (constant throughout the domain).

Figure 1 shows layer-averaged CCN spectra calculated at various heights after 120 min of simulation time, when the dynamical fields are approximately in steady state. Spectra at 900 m are above the cloud and indicate the background CCN spectrum; those at 700 m lie in-cloud, and those at 400 m lie just below cloud. Figure 1a is for the run which employs the R_{logn} regeneration scheme, while Figure 1b is for the R_{act} scheme, as defined in section 2. Figure 1c represents results from a simulation with the three-moment scheme R_{logn3} which carries aerosol number, mass, and surface area; here, the standard deviations of the regenerated lognormal spectra are not fixed, and fluctuate according to the ratio of the regenerated mass, number, and surface area.

It is immediately apparent that the R_{logn} scheme creates a bimodality in the CCN spectrum that is not entirely removed when a third moment is carried, whereas the R_{act} scheme conserves the spectral form (except, of course, within the cloud layer, where the average shown is for a region depleted in CCN). Note that all schemes conserve total mass and number, and hence regenerate the correct global mass mean diameter for the aerosol. The creation, however, of a second mode in the R_{logn} scheme is an undesirable feature since it affects subsequent activation events and obscures possible evidence of bimodality related to a physical process rather than a numerical artifact. Given the fact that the three-moment scheme requires significantly more computational time and memory, and in the absence of any clear advantage, R_{act} has been chosen in subsequent simulations.

3.2. Experiments Including Collision-Coalescence

Our baseline experiment uses the initial conditions outlined in section 2.4, together with an initial lognormal CCN spectrum with N = 50 cm^{-3}, r_g = 0.08 μm, and, σ = 1.8 throughout the domain. A sample of dynamical and microphysical fields after 120-min simulation time is shown in Figure 2. Figure 2a shows the boundary layer vertical velocity structure, which exhibits maxima and minima on the order of 1 m s^{-1}. The cloud water field r_l (Figure 2b) exhibits a solid cloud deck (which remains so throughout the run), a linear increase with height, and peak values of 0.5 g kg^{-1}. Drop concentrations N_d (Figure 2c) exhibit the classical "constant with height" profile commonly observed in marine stratocumulus [e.g., *Nicholls*, 1984]. Finally, Figure 2d shows that the CCN number concentration is most strongly depleted in the updrafts, and

less so in the downdrafts. Downdraft regions tend to advect lower concentrations of CCN into the subcloud layer.

Figure 3 examines layer-averaged profiles of drop spectra after 120 min at a few select heights. Figure 3a is for the number distribution (derived from N_k divided by bin width), while Figure 3b is for the mass distribution (derived from M_k/bin width). Superimposed on the drop spectra are the solute distribution functions, (i.e., S_k/bin width; [g cm^{-4}]). The spectrum is dominated by a mode of cloud droplets, but clear evidence of a second collision-coalescence related mode is evident. Note how the solute distribution scales with the drop spectrum [e.g., *Flossmann et al.*, 1985]; at the small drop end where the dominant processes are activation and condensation, solute scales with drop number; at the large drop end, where collision-coalescence is the dominant growth process, solute scales with drop mass due to the mass dependence of the growth kernels.

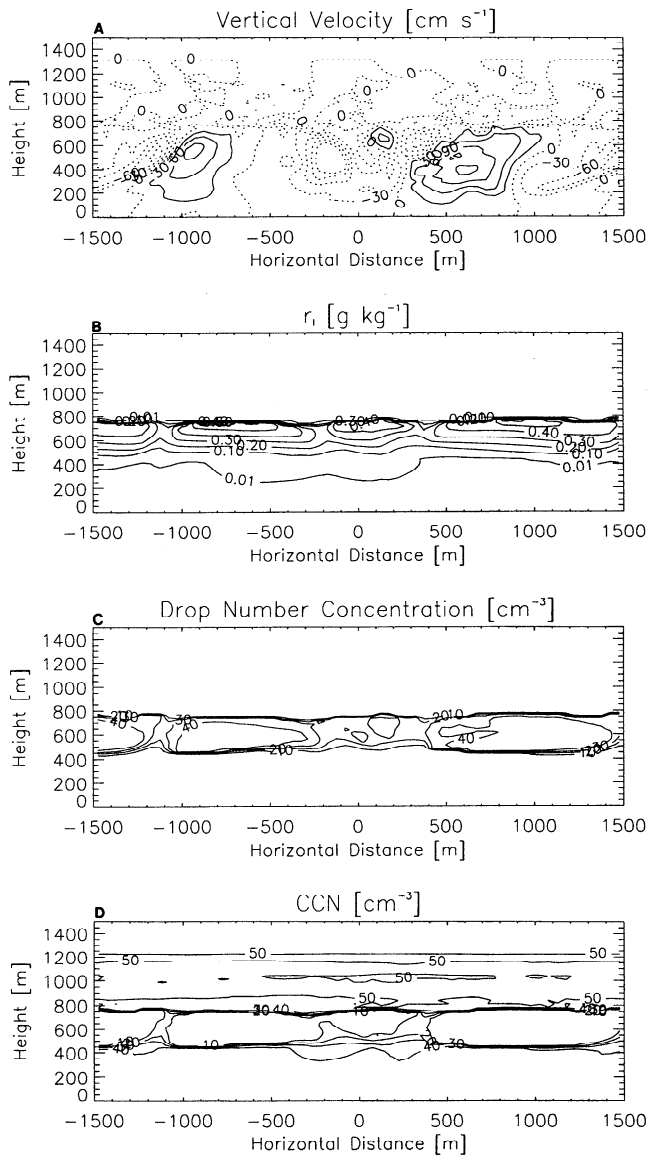

Figure 2. Contour plots at 120 min for the base case (including collision-coalescence): (a) the vertical velocity field, (b) liquid-water mixing ratio r_l, (c) drop number concentration N_d; and (d) CCN concentration N_a.

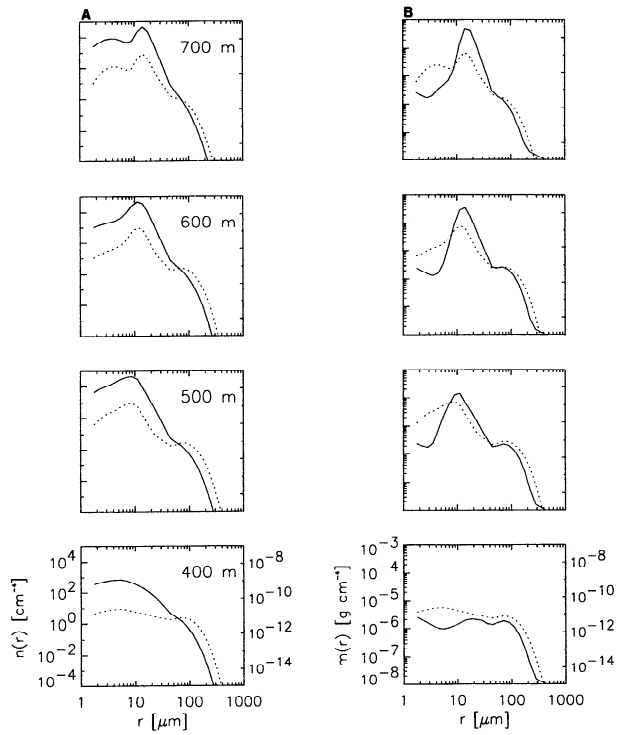

Figure 3. Layer averaged drop spectra at select heights both in-cloud (500 m, 600 m, 700 m) and below cloud (400 m) after 120 min. Figure 3a indicates the drop number distribution (solid line) superimposed on the solute mass distribution (dotted line); Figure 3b indicates the drop mass distribution (solid line) superimposed on the solute mass distribution. Note that for small drops, solute mass scales with drop number while for large drops, solute mass scales with drop mass.

In Figure 4 the time evolution of a number of domain-averaged fields is shown. Turbulence, as represented by the root-mean-square velocity, w_{rms}, shows a buildup from an initially quiescent boundary layer (BL), achieves a maximum at about 50 min, and thereafter relaxes to an approximately steady state. The cloud-water field r_l has a fairly steady value of about 0.25 g kg^{-1}. In contrast to this, the drop number concentration N_d peaks at about 40 cm^{-3}, then declines steadily during the course of the run as a result of collision-coalescence. After 3 hours, drop number concentration is on the order of 16 cm^{-3}, representing a depletion of 60%. Figure 5 shows the temporal evolution of the domain averages of the total number concentration of CCN, N_t, and the total mass concentration, M_t, where N_t comprises both unactivated CCN

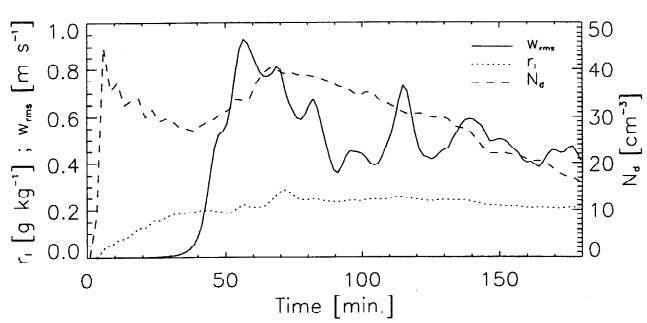

Figure 4. Temporal evolution of averaged fields: w_{rms} (averaged over the boundary layer), r_l and N_d (cloud averages).

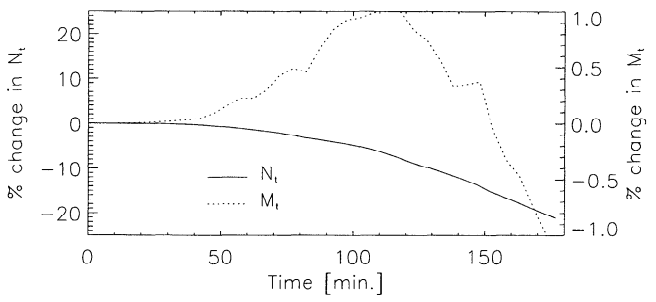

Figure 5. Temporal evolution of domain averages of total number (unactivated CCN + drops) and total mass (unactivated CCN + solute) for the base case including collision-coalescence.

and drop number, and M_t is the sum of dry CCN mass plus solute. Although M_t is approximately constant with time (maximum error is on the order of 1%), N_t decreases steadily and is depleted by 25% over the course of the run. In an ideal model, M_t should be conserved absolutely; the excursions observed here are a result of an imperfect model formulation; although the advection scheme [*Stevens et al.*, 1996], and the turbulent diffusion scheme both conserve mass, their combined effect may not be conservative. In addition, time-stepping a pressure-like variable according to an approximate equation (as is done in this model and other pseudo-compressible models) does not force mass conservation. The result is the small apparent mass source evident in Figure 5. Conservation of number in the absence of collision-coalescence and sedimentation is on the order of about 0.2%. The greater error in M_t results from the advection of the extra 25 scalars representing S_k.

In Figure 6 layer-averaged CCN spectra are shown after 120 min at a few select model levels. Figure 6a is an average over the entire layer; Figure 6b is an average over updrafts; and Figure 6c is an average over downdrafts. Spectra below the cloud are mostly unperturbed, while those within the cloud (level 700 m) exhibit a slight bimodality at about 0.2-μm radius. If one superimposes the averaged spectrum in the region below cloud on the background spectrum, one sees that collision-coalescence processing has reduced the CCN concentration near the mode, and has increased the number of particles greater than about 0.2-μm radius (Figure 7).

4. Discussion

In a marine stratocumulus cloud, one can expect both physical processing through collision-coalescence and chemical processing via aqueous phase chemistry to be occurring simultaneously; the effect of the former, as shown here, is a decrease in CCN concentration without change in total mass, while the effect of the latter is an increase in CCN mass without change in number. Consider a CCN spectrum represented by total mass M_a and total number N_a, quantities integrated over the size distribution. The mass-mean radius of this spectrum r_a is given by

$$r_a \propto \left(\frac{M_a}{N_a}\right)^{1/3}. \tag{5}$$

For small changes, it follows that

$$\frac{\delta r_a}{r_a} \approx \frac{1}{3}\frac{\delta M_a}{M_a} \tag{6a}$$

$$\frac{\delta r_a}{r_a} \approx -\frac{1}{3}\frac{\delta N_a}{N_a}. \tag{6b}$$

Thus, collision-coalescence is potentially as significant a forcing on the size distribution of CCN as aqueous phase chemistry. In the subsequent discussion an attempt is made to evaluate the relative importance of these forcings given the time available for processing in a stratocumulus-capped boundary layer. For the purposes of such comparisons, it is demonstrated that box model results can be averaged, using appropriate trajectory information, to yield time-dependent drop number depletions that compare quantitatively with those obtained in the full MBL simulations described above. This result is very useful in that it permits the exploration of the effects of collision-coalescence for a larger parameter space, and also permits examination of chemical processing in this simpler box model framework.

4.1. Relating Collision-Coalescence Processing to CCN Processing

Results presented in section 3 suggest that the stratocumulus cloud in our case study may be able to reduce cloud drop concentrations by about 60% over the course of 3 hours. This depletion is not related to precipitation; in fact, an attempt has been made to simulate a case in which there is no (or negligible) loss to precipitation. This depletion in cloud drop number can be related to a depletion in the CCN concentration as follows. Defining the total concentration of CCN by N_a, and of drops by N_d, it follows that N_a after time t (i.e., after collision-coalescence processing) relative to N_a in the initial state is given by

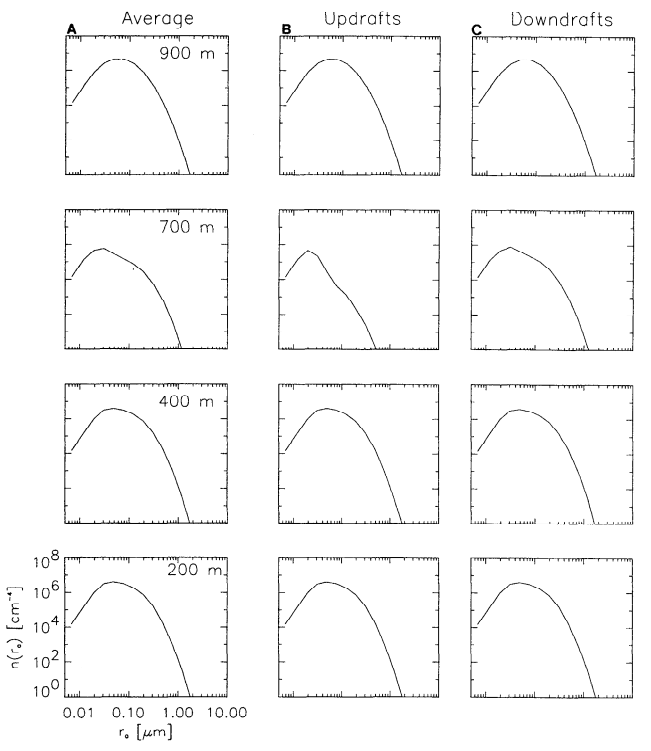

Figure 6. Averaged CCN spectra at select heights for the base case after 120 min: (a) layer average, (b) average over updrafts, (c) average over downdrafts.

$$\frac{N_a(t)}{N_a(0)} = \frac{(N_a(0) - N_d(0)) + d(t)\,N_d(0)}{N_a(0)}, \tag{7}$$

where $N_d(0)$ is the number of drops initially activated and $d(t)$ is $N_d(t)/N_d(0)$, the ratio of the drop number at time t to that at time 0. We define $D(t) = 1 - d(t)$ as the degree to which cloud droplet concentration has been depleted; if $D = 0$, there is no depletion, while if $D = 0.5$, drop concentrations have been reduced to half of their original value. Equation (7) reduces to

$$\frac{N_a(t)}{N_a(0)} = 1 - D(t)\,\frac{N_d(0)}{N_a(0)}. \tag{8}$$

This depletion in N_a can be related to the change in particle radius using (6b):

$$\frac{r_a(t)}{r_a(0)} = \left[1 - D(t)\,\frac{N_d(0)}{N_a(0)}\right]^{-1/3}. \tag{9}$$

Equation (9) shows that in order to impact the mean radius for the entire population, r_a, through collision-coalescence processing, it is necessary that there be a high degree of depletion (large D), and also that the process be working on a significant fraction of available CCN ($N_d(0)/N_a(0)$ close to unity). Note that a larger impact is expected if an increase in the mean size of only those particles that were activated were computed. In this sense the following calculations may be regarded as conservative.

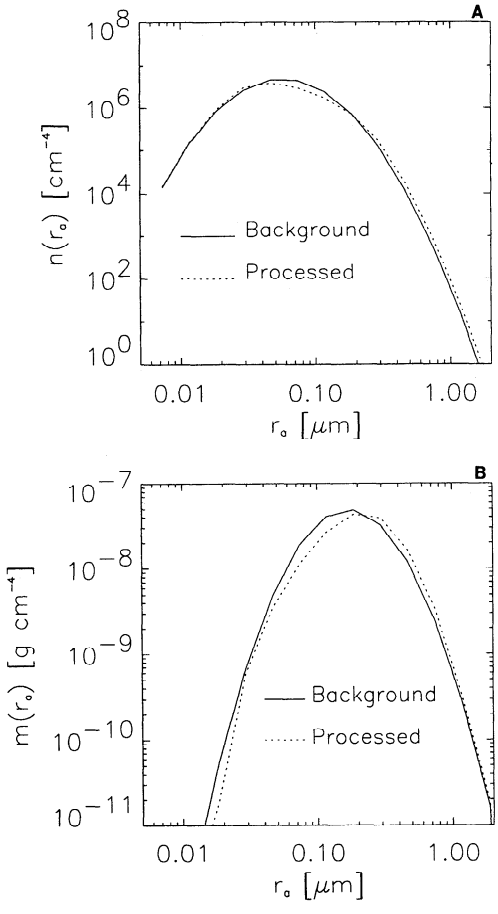

Figure 7. Average subcloud CCN spectra (dashed line) superimposed on the background CCN size spectrum (solid line) after 120 min: (a) the number distribution, (b) the mass distribution. Processed spectra indicate a shift to larger sizes.

Table 1. Depletion Factors $D(t)$ (%) and Percentage Increase in Particle Radius Based on the Eddy-resolving Model Simulation

Time, min	$D(t)$	$100 \times [r_a(t)/r_a(0) - 1]$
60	0	0
90	8.5	2.4
120	22.5	6.8
150	44.2	15.7
180	61.0	25.0

In Table 1, values of $D(t)$ (expressed as percent) computed at several times during the simulation presented in section 3 are shown, together with estimates of $r_a(t)/r_a(0)$ for the average $N_d(0)/N_a(0)$ of 0.8. It is noted that the impact of collision-coalescence in this case is substantial. For example, for $D = 44\%$ (achieved at 150 min), the mean radius has increased by 15.7%. Note the reasonable consistency of this estimate with the averaged CCN spectra shown in Figure 7b, where the shift in mean radius is calculated as 18%. For a sodium chloride particle, this change is equivalent to shifting the critical supersaturation for the mean particle size from 0.013% to 0.010%, implying a feedback of this process to the subsequent cloud evolution; this aspect will be discussed further in section 5. These estimates of the impact on the aerosol spectrum are based on domain averages of the extent of depletion, but are nevertheless useful for calculation of first-order effects. In addition, these simple equations can be applied to other systems, if a means for estimating $D(t)$ is available, since one can estimate $N_d(0)$ from the typical cloud supersaturation and the CCN activation spectrum. In the following subsection methods of determining $D(t)$ are examined.

4.2. Time Available for Processing: Trajectory Analyses

One of the most important factors in this discussion of the relative effects of collision-coalescence and aqueous phase chemistry is how much time is available for processes to act. Although stratocumulus decks are persistent for hours and even days, the relevant timescale is the time that a typical air-parcel trajectory spends in cloud. The results of *Stevens et al.* [1996], who used the same numerical model as in this study, are applied to estimate this timescale. These authors analyzed large eddy simulations of the cloud-capped marine boundary layer by following parcel trajectories and calculating the PDF of the amount of time that parcels spent in cloud during the course of 1 hour. Those results are reproduced here in Figure 8. First, it is noted that the PDF associated with the two-dimensional run is different from its three-dimensional counterpart; the latter shows that a small number of trajectories may spend as much as 40-min per hour in-cloud. More typical in-cloud residence times are on the order of 12 min (the mean for the three-dimensional PDF). *Pruppacher and Jaenicke* [1995] have used globally averaged values to estimate the time spent by air parcels in various cloud types. For stratus and stratocumulus, this value is 3.1 hours. The mean in-cloud residence time of 12 min h^{-1} in Figure 8 implies an average stratus/stratocumulus cloud lifetime of 15.5 hours. This value is a reasonable estimate, given observed diurnal variations and persistence of Sc. Using these PDFs, which are defined as $f(t)$,

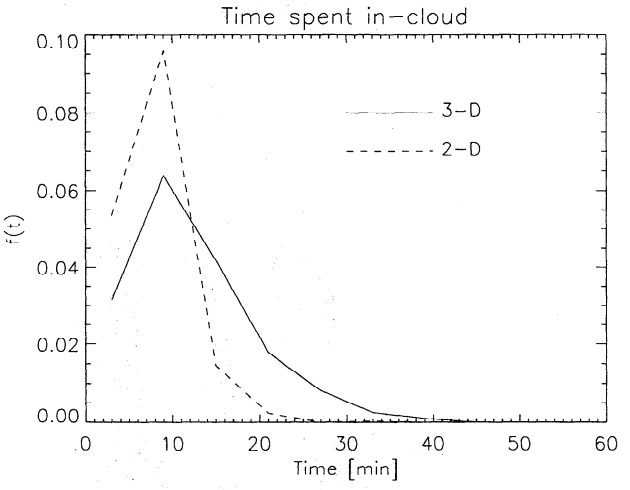

Figure 8. Probability distribution functions (PDFs) of parcel in-cloud residence time based on trajectory analyses during the course of one hour's simulation (adapted from *Stevens et al.* [1996]).

representative values of drop number depletion are calculated using the integral average formula

$$\bar{D} = \frac{\int f(t)\,D(t)\,dt}{\int f(t)\,dt}. \tag{10}$$

Using box model calculations of collision-coalescence only, depletion factors $D(t)$ have been calculated at times corresponding to those in the trajectory analyses and for fixed values of N_d and r_l. Then, (10) has been used to calculate $\bar{D}$ representing the average depletion over the course of an hour. It is seen (Figure 9) that results are strongly dependent on both N_d and r_l, and that simulations using three-dimensional trajectories have an enhanced depletion compared to the two-dimensional simulations (cf. Figures 9a and 9b). Despite the fact that both PDFs have the same modal value, the three-dimensional PDF has a "tail" out to longer times (Figure 8), which has a strong impact on the calculations.

Next, the box model collision-coalescence simulations are compared with the drop depletions observed in the MBL simulations presented in section 3. From Figure 9, for $N_d = 40$ cm^{-3} and $r_l = 0.25$ (the cloud-average values reported in Figure 4 at 60 min), the average depletion $\bar{D}$ is on the order of 10% for a three-dimensional simulation and 5% for a two-dimensional run. These depletion factors are somewhat smaller than that directly determined from the MBL simulation output (Table 1) between 60 and 120 min, namely 22.5%. The reasons for this are multifold: (1) Use of the average r_l of 0.25 g kg^{-1} is probably inappropriate since the trajectories that spend the most time in cloud, and the ones responsible for most of the collision-coalescence, tend to have rather flat trajectories near cloud top [*Stevens et al.*, 1996], where r_l is on the order of 0.5 g kg^{-1}. Using $r_l = 0.4$, and $N_d = 40$ cm^{-3} yields $\bar{D}$ of 30% for a three-dimensional simulation and 20% for a two-dimensional run, much closer to the value of 22.5% in Table 1. Clearly, the convolution of path-dependent liquid-water content together with $f(t)$ is not easily represented by a simple calculation of this type. (2) The estimates shown in Figure 9 should be regarded as conservative since only collision-coalescence growth is allowed; condensational growth will assist in the production of larger drops and expedite the onset of collision-coalescence. (3) Results in Figure 9 are sensitive to the assumed breadth of the distribution in the initial drop spectrum. These values were obtained for a lognormal spectrum with a σ of 1.5, derived from a fitting lognormal spectra to the drop spectra produced by the model, and not very different from the value of 1.42 used by *Nakajima and King* [1990]. The occurrence of broader spectra, especially in the higher r_l regions, would serve to enhance collision-coalescence as well as $\bar{D}$. Indeed, near cloud top, values of 2 are not uncommon in the model run. (4) The eddy-resolving model results include an accumulative effect which is not included in the box model runs. As the model evolves, CCN are slowly depleted, and cloud drop concentrations become slowly, but progressively smaller, so that collision-coalescence is constantly being enhanced.

Despite these limitations, the box model results, in conjunction with information on parcel trajectory PDFs, provide an adequate framework for evaluating processing timescales, and this technique will be employed to compare the relative effects

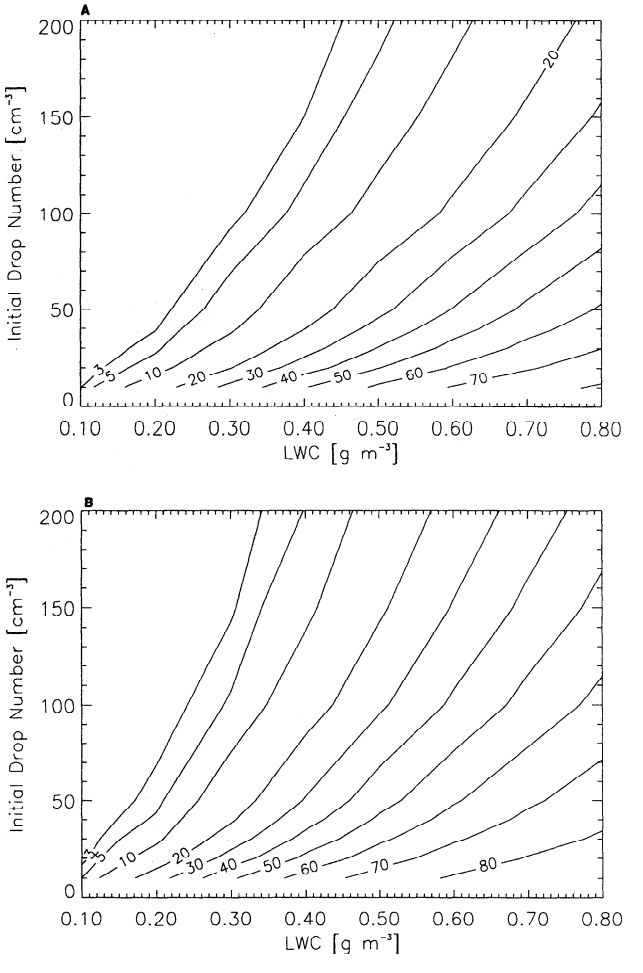

Figure 9. Contour plots of average depletion $\bar{D}$ expressed as a percent for different liquid water content and N_d calculated using equation (10) with $f(t)$ defined by the PDFs in Figure 8, and a box model calculation of collision-coalescence; (a) using PDFs derived from a two-dimensional simulation; and (b) using PDFs derived from a three-dimensional simulation.

of collision-coalescence and the addition of aerosol mass via aqueous phase chemistry. For purposes of this comparison, (9) was used to relate the drop depletions in Figure 9 to changes in mean particle size; the results are reported in Table 2. The impact upon radius is highly variable, ranging from negligible to on the order of a 10% change over the course of 1 hour of processing.

4.3. Timescales for Aqueous Chemistry Processing

The degree to which the aqueous phase addition of mass impacts aerosol spectra has been discussed at length by *Hoppel et al.* [1989], who proposed this as a mechanism to create the bimodal aerosol spectra frequently observed in the marine boundary layer. Their hypothesis is that repeated cycling of aerosol through nonprecipitating clouds deposits sulfate mass onto those particles activated in "typical" marine cumulus environments (i.e., those larger than about 0.06 μm in radius). The particles resuspended upon evaporation of the drops have been grown to larger size, and eventually form a separate, larger mode at about 0.09 μm, that is distinguishable from smaller particles that are not active as CCN at those supersaturations. In their analysis, they assumed long timescales to examine the cumulative effect of the aqueous phase mass addition process; here, the effects of this process will initially be examined on a shorter timescale, consistent with the timescales selected for the collision-coalescence process.

Estimates using reaction timescales from *Chameides* [1984]. The methodology discussed in section 4.2 is now employed to evaluate the effects of in-cloud residence times upon the extent of aqueous phase conversion of SO_2 (S[IV]) to sulfate (S[VI]). The conceptual model is that of air parcels, with specified initial gas phase concentrations of SO_2, introduced into the cloud layer during the course of their trajectories. In the presence of liquid-water, the SO_2 dissolves into the drops and undergoes rapid oxidation, the extent of which is limited not only by the in-cloud residence time, but also by the chemical environment; for example, the conversion may be impacted by the gaseous concentrations of oxidants, or by the pH of the droplets. Similar to the equation applied to compute the extent of drop depletion, representative values of the extent of chemical conversion, $\bar{c}$, are calculated as follows:

$$\bar{c} = \frac{\int f(t)c(t)\,dt}{\int f(t)\,dt}. \tag{11}$$

Table 2. Percentage Increase in Particle Radius Based on $\bar{D}$ in Figure 9 and Equation (9) With $N_d(0)/N_a(0) = 0.8$

	Two-dimensional, N_d [cm^{-3}]		Three-dimensional, N_d [cm^{-3}]	
LWC, g m^{-3}	50	100	50	100
0.1	0.08	0.03	0.13	0.05
0.2	0.54	0.19	1.09	0.35
0.5	8.60	3.54	16.7	8.93

Results represent 1 hour of cloud processing. LWC is liquid water content.

Table 3. Percentage Conversion of SO_2 to Sulfate per Hour Based on the PDFs in Figure 8, and Equation (11) and the Results of *Chameides* [1984]

LWC, g m^{-3}	$\bar{c}$, Two-dimensional	$\bar{c}$, Three-dimensional
0.1	11	17
0.2	28	37
0.5	45	54

PDF is probability distribution function.

Here, $c(t)$ is the extent of chemical conversion at a time t, which has been estimated using the results of *Chameides* [1984]. In his study, he determined the percent conversion of S[IV] to S[VI] as a function of time for ambient conditions representative of a marine stratiform cloud. The percent conversion increases as cloud liquid-water content is increased, and decreases as initial SO_2 concentrations are increased. In the latter case, the rate of oxidation for initial SO_2 concentrations above about 1 ppbv was inhibited by the depletion of the oxidant hydrogen peroxide; however, total mass converted to S[VI] over a time period, the quantity of interest here, can still be appreciably larger than that computed for lower initial gas phase levels.

In Table 3, values of $\bar{c}$ computed for the two-dimensional and three-dimensional in-cloud PDFs are reported for three values of liquid-water content LWC corresponding to those used by *Chameides* [1984]. (We use LWC [g m^{-3}] rather than r_l [g kg^{-1}] in order to be consistent with the discussion in *Chameides* [1984]. The difference between LWC and r_l is on the order of 10% given that the in-cloud air density is about 1.1 10^{-3} g cm^{-3}.) For the case of LWC = 0.5 g m^{-3}, the percent conversion was reported as a function of time in his Figure 7. For the other choices of LWC, the percent conversions reported in his Table 4 for selected simulation times were interpolated to other times as needed for use in (11). Thus these estimates are only approximate. The initial gas phase concentration of SO_2 used in his base case studies was 55 pptv, consistent with clean marine values estimated by other authors [e.g., *Toon et al.*, 1987]; this value was adopted for the calculations reported here.

Using these values of $\bar{c}$, the mass of S[VI] produced in the droplets during 1 hour may be computed. The addition of this mass, M_{aq}, to the CCN spectrum is related to an increase in the mean size by

$$\frac{r_a(t)}{r_a(0)} = \left[1 + \frac{M_{aq}(t)}{M(0)}\right]^{1/3}. \tag{12}$$

Results of this calculation are summarized in Table 4. The initial aerosol mass was determined from the number concentration indicated, a geometric mean radius of 0.08 μm, and a geometric standard deviation of 1.8, as used in the MBL simulation. The change in mean size attributable to chemistry alone (Table 4) may be compared to that for physical processing alone (Table 2). The effects upon radius increase with LWC for both processes, but the rate of increase is much greater for the collision-coalescence mechanism. Aqueous chemistry produces noticeable effects (a few percent change in size) for the low LWC value, whereas collision-coalescence has a negligible effect upon mean size for low liquid-water contents. In contrast, the impact of collision-coalescence is com-

Table 4. Percentage Increase in Particle Radius Based on $\bar{c}$ in Table 3 and Equation (12) for Base Case Lognormal Aerosol

	Two-dimensional, N_a [cm^{-3}]		Three-dimensional, N_a [cm^{-3}]	
LWC, g m^{-3}	50	100	50	100
0.1	0.78	0.39	1.16	0.58
0.2	1.89	0.96	2.49	1.26
0.5	3.01	1.53	3.59	1.83

Base case lognormal aerosol with $r_g = 0.08$ μm and an initial SO_2 concentration of 55 pptv. Results represent 1 hour of cloud processing. Note that N_a is varied in order to increase initial particle mass.

parable to or larger than that of chemistry for LWC $\geq$ 0.5 g m^{-3}.

Bower and Choularton [1993] and *Flossmann* [1994] have also investigated the role of short-term processing of aerosol for hill cap clouds and precipitating cumulus, respectively. The work of *Bower and Choularton* focused on chemical processing only, while that of *Flossmann* included both chemical processing as well as collision-coalescence. In the latter study, the effect of collision-coalescence on the CCN spectrum was noted, but not quantified; quantification would have been difficult due to the occurrence of precipitation. The different nature of these cloud types from the stratocumulus clouds simulated in this work, together with the sensitivity to environmental parameters used in those studies makes quantitative comparison difficult. Nevertheless, it is noteworthy that the estimates of processing in Tables 2 and 4 are not inconsistent with those in the above-mentioned works.

The results in Table 2 through Table 4 consider only a small subset of the conditions for aqueous phase chemistry and physical processing that may exist in the atmosphere, and the relative importance of the two mechanisms may vary substantially depending upon these conditions. These results do, however, suggest that the impacts of collision-coalescence on the CCN spectrum regenerated from nonprecipitating clouds can, under some circumstances, be as substantial as those resulting from aqueous phase production of particulate mass. Both processes increase the mean size and thereby enhance the cloud-nucleating activity of the CCN in subsequent cloud cycles. Further, collision-coalescence represents a means of reducing particle number concentrations in addition to affecting mean size, and thus could assist in reducing high number concentrations of particles advected from continental regions (on the order of 1000's cm^{-3}) to observed lower values over marine regions (on the order of 100s cm^{-3}) [*Hudson*, 1993].

Relationship between chemistry timescales examined here and longer-term averages. The estimates of percent conversion of S[IV] to S[VI] in cloud, reported in Table 3, should be consistent with other estimates of the rate of the aqueous pathway for oxidation of gaseous sulfur species. In examining the effect of chemistry on the aerosol distribution, *Hoppel et al.* [1989] used steady state, boundary-layer sulfur mass budget arguments (based on dimethylsulfide [DMS] as the primary sulfate precursor) to develop timescale estimates. The mass addition rate used in their work, 2.5×10^{-18} g cm^{-3} s^{-1}, is lower than those derived in the present study by factors of 3 to 15. Also, the study of the marine sulfur cycle by *Toon et al.* [1987] deduced mass conversion rates, attributed to unspecified heterogeneous chemical pathways which include aqueous chemistry in droplets, of about 4% per hour; *Kritz* [1982] derived values of 2–4% per hour for the marine boundary layer with cumulus. Both of these estimates are significantly lower than even our lowest hourly conversion rate of 11%. These apparent discrepancies can be reconciled by recognizing that, whereas the present study considers a single cloud-cycling event of at most a few hours' duration, budget studies of necessity average over longer time periods to deduce total source and sink rates of the species. Thus, the budget studies weight the overall conversion by the frequency of occurrence and persistence of cloud cover.

The two approaches may be reconciled by extending the hourly mass conversion estimates over longer time periods, using assumed cloud frequency distributions. *Pruppacher and Jaenicke* [1995] suggest an areal cloud coverage for stratus/stratocumulus of 23% based on the data of *Warren et al.* [1986]; this may alternatively be interpreted as the presence of such cloud for 23% of the time, on average. Applying this fraction to the 11% h^{-1} conversion derived here, an overall conversion rate of 2.5% h^{-1} is obtained, in excellent agreement with earlier studies. The areal coverage of Cu is estimated as 7% by *Pruppacher and Jaenicke* [1995]; applied to our highest conversion rates of 54% h^{-1}, overall conversions near 4% h^{-1} are obtained. The 7–23% areal cloud coverages also account for factors of 4 to 14 in the hourly versus longer-term rates, bringing our mass addition rate estimates closer to that used by *Hoppel et al.* [1989], with additional unaccounted-for differences attributable to our assumed gas phase SO_2 concentration. These comparisons are not meant to be completely quantitative, but to show that the different estimates obtained by examining processing on short and long timescales can be reconciled by invoking reasonable estimates of regional cloud coverage. This observation implies that the rate of change of mean particle size due to aqueous phase mass addition may be substantially underestimated if steady state mass budget arguments are used. Our results suggest that significant modification of the aerosol size spectrum can occur during one cloud cycle, and that this conclusion is based on rapid mass addition rates that are nonetheless consistent with longer-term averaged ones.

5. Summary and Conclusions

A two-dimensional eddy-resolving model of the stratocumulus-capped marine boundary layer has been presented. The model is coupled with a microphysical model that explicitly resolves the drop and CCN spectra, and allows for solute transfer between drop bins. The model is used to evaluate cloud processing of the CCN spectrum through the collision-coalescence process for a case where precipitation removal is minimal. In order to extend the validity of these results, trajectory analyses of parcel in-cloud residence times derived by *Stevens et al.* [1996] have been used together with box model calculations of collision-coalescence to explore the parameters affecting processing through collision-coalescence. This trajectory information is then used to deduce the extent of in-cloud conversion of SO_2 to sulfate.

The simple analyses reported here place some bounds on the degree to which a persistent stratocumulus layer cloud of about 300 m depth can impact the aerosol spectrum, and in addition, compare the relative importance of physical and chemical processing under some marine-type conditions. Collision-

coalescence increases the mean size of the CCN regenerated from a nonprecipitating cloud by reducing the number concentration and maintaining constant mass. This effect is small, but measurable. Aqueous phase chemistry, on the other hand, also increases particle size, but does so via the addition of particulate mass to a constant number concentration. The results shown here suggest that the two mechanisms may produce comparable rates of increase in the mean particle size under certain conditions. In particular, aqueous phase chemistry may have a greater impact at lower cloud liquid-water contents, whereas collision-coalescence can produce substantial changes on short timescales at higher r_l, or for broader drop spectra.

An interesting inference is that the collision-coalescence mechanism will tend to accelerate during a cloud cycle. This is because the increase in particle size reduces the critical supersaturation of the particle, making it a more effective CCN [*Hudson*, 1993; *Flossmann*, 1994]; further, depletion of the CCN number concentration results in the formation of larger droplets since there are fewer condensation sites available, and these larger droplets have faster collision-coalescence rates. In contrast, the rate of aqueous phase chemistry is not expected to accelerate, and is instead likely to slow down during a cloud cycle. As gaseous reactants are depleted, the rate of reaction slows, and the overall conversion of species may in fact be limited by the consumption of one or more reactants. Also, aqueous phase chemical reactions such as the conversion of S[IV] to S[VI] produce acidic species, decreasing the pH of the cloud water and reducing solubility as well as the rates of some pH-sensitive reactions. These observations suggest that the relative importance of physical and chemical processing may also vary with time during a cloud cycle.

In order to focus on the impact of collision-coalescence on the CCN spectrum, the current model has ignored a number of aerosol processes such as impaction scavenging, new particle sources, and particle coagulation. The neglect of concurrent, coupled gas and aqueous phase chemistry calculations means that the results presented here are in some respects tentative. Nevertheless, they are useful in that they place some bounds on the extent of processing through collision-coalescence and provide a baseline for future work that will address a more comprehensive number of variables.

Acknowledgments. The authors wish to acknowledge useful discussions with Wendy Richardson. This study has been partially supported by the NOAA Climate and Global Change Program, the National Science Foundation under grant ATM-9215951 and by the Office of Naval Research under grants N00014-93-0420-P00001 and N00014-93-F0029.

References

Ackerman, A. S., O. B. Toon, and P. V. Hobbs, A model for particle microphysics, turbulent mixing, and radiative transfer in the stratocumulus-topped marine boundary layer and comparisons with measurements, *J. Atmos. Sci.*, *52*, 1204–1236, 1995.

Albrecht, B. A., Aerosols, cloud microphysics, and fractional cloudiness, *Science*, *245*, 1227–1230, 1989.

Baker, M. B., and R. J. Charlson, Bistability of CCN concentrations and thermodynamics in the cloud-topped boundary layer, *Nature*, *345*, 142–145, 1990.

Betts, A. K., and R. Boers, A cloudiness transition in a marine boundary layer, *J. Atmos. Sci.*, *47*, 1480–1497, 1990.

Bower, K. N., and T. W. Choularton, Cloud processing of the cloud condensation nucleus spectrum and its climatological consequences, *Quart. J. R. Meteorol. Soc.*, *119*, 655–679, 1993.

Chameides, W. L., The photochemistry of a remote marine stratiform cloud, *J. Geophys. Res.*, *89*, 4739–4755, 1984.

Chen, C., and W. R. Cotton, A one-dimensional simulation of the stratocumulus-capped mixed layer, *Boundary Layer Meteorol.*, *25*, 289–321, 1983.

Chen, J. P., and D. Lamb, Simulation of cloud microphysical and chemical processes using a multicomponent framework, I, Description of the microphysical model, *J. Atmos. Sci.*, *51*, 2613–2636, 1994.

Cotton, W. R., B. Stevens, G. Feingold, and R. L. Walko, Large eddy simulation of marine stratocumulus cloud with explicit microphysics, paper presented at the ECMWF/GCSS Workshop on Parameterization of the Cloud Topped Boundary Layer, Eur. Cent. Meteorol. Weather Forecasts, Reading, United Kingdom, June 8–11, 1993.

Feingold, G., B. Stevens, W. R. Cotton, and R. L. Walko, An explicit cloud microphysical/LES model designed to simulate the Twomey effect, *Atmos. Res.*, *33*, 207–233, 1994.

Feingold, G., B. Stevens, W. R. Cotton, and A. S. Frisch, On the relationship between drop in-cloud residence time and drizzle production in numerically simulated stratocumulus clouds, *J. Atmos. Sci.*, *53*, 1108–1122, 1996.

Flossmann, A. I., A 2-D spectral model simulation of the scavenging of gaseous and particulate sulfate by a warm marine cloud, *Atmos. Res.*, *32*, 233–248, 1994.

Flossmann, A. I., W. D. Hall, and H. R. Pruppacher, A theoretical study of the wet removal of atmospheric pollutants, I, The redistribution of aerosol particles captured through nucleation and impaction scavenging by growing cloud drops, *J. Atmos. Sci.*, *42*, 582–606, 1985.

Garrett, T. J., and P. V. Hobbs, Long-range transport of continental aerosols over the Atlantic ocean and their effects on cloud structures, *J. Atmos. Sci.*, *52*, 2977–2984, 1995.

Hegg, D. A., and P. V. Hobbs, Measurements of sulfate production in natural clouds, *Atmos. Environ.*, *16*, 2663–2668, 1982.

Hegg, D. A., L. F. Radke, and P. V. Hobbs, Particle production associated with marine clouds, *J. Geophys. Res.*, *95*, 13,917–13,926, 1990.

Hoppel, W. A., J. W. Fitzgerald, G. M. Frick, R. E. Larson, and E. J. Mack, Atmospheric aerosol size distributions and optical properties found in the marine boundary layer over the Atlantic ocean, *NRL Rep. 9188, NTIS-ADA 210800*, Nav. Res. Lab., Washington, D. C., 1989.

Hudson, J. G., Cloud condensation nuclei near marine cumulus, *J. Geophys. Res.*, *98*, 2693–2702, 1993.

Kritz, M. A., Exchange of sulfur between the free troposphere, marine boundary layer, and the sea surface, *J. Geophys. Res.*, *87*, 8795–8803, 1982.

Kogan, Y. L., D. K. Lilly, Z. N. Kogan, and V. V. Filyushkin, The effect of CCN regeneration on the evolution of stratocumulus layers, *Atmos. Res.*, *33*, 137–150, 1994.

Mitra, S. K., H. R. Pruppacher, and J. Brinkmann, A windtunnel study on the drop-to particle conversion, *J. Aerosol Sci.*, *23*, 245–256, 1992.

Mordy, W. A., Computations of the growth by condensation of a population of cloud droplets, *Tellus*, *11*, 16–44, 1959.

Nakajima, T., and M. D. King, Determination of the optical thickness and effective particle radius of clouds from reflected solar radiation measurements, I, Theory, *J. Atmos. Sci.*, *47*, 1878–1893, 1990.

Nicholls, S., The dynamics of stratocumulus, *Quart. J. R. Meteorol. Soc.*, *110*, 821–845, 1984.

Paluch, I. R., and D. H. Lenschow, Stratiform cloud formation in the marine boundary layer, *J. Atmos. Sci.*, *48*, 2141–2158, 1991.

Pielke, R. A., et al., A comprehensive meteorological modeling system—RAMS, *Meteorol. Atmos. Phys.*, *49*, 69–91, 1992.

Pruppacher, H. R., and R. Jaenicke, The processing of water vapor and aerosols by atmospheric clouds, a global estimate, *Atmos. Res.*, *38*, 283–295, 1995.

Richardson, W. A., S. M. Kreidenweis, and W. R. Cotton, Cloud processing of aerosol using a hybrid LES/PARCEL model with solute-following microphysics, M.S. thesis, Colo. State Univ., Dep. Atmos. Sci., Boulder, 1995.

Stevens, B., G. Feingold, W. R. Cotton, and R. L. Walko, On elements of the microphysical structure of numerically simulated stratocumulus, *J. Atmos. Sci.*, *53*, 980–1006, 1996.

Toon, O. B., J. F. Kasting, R. P. Turco, and M. S. Liu, The sulfur cycle in the marine atmosphere, *J. Geophys. Res.*, *92*, 943–963, 1987.

Trautmann, T., On the stochastic approach to the kinetics in polydisperse multicomponent populations, *Atmos. Res.*, *29*, 99–113, 1993.

Turco, R. P., P. Hammill, O. B. Toon, R. C. Whitten, and C. S. Kiang, The NASA Ames Research Center stratospheric aerosol model, I, Physical processes and computational analogs, *NASA TP*, *1362*, 94, 1979.

Twomey, S., Pollution and the planetary albedo, *Atmos. Environ.*, *8*, 1251–1256, 1974.

Twomey, S., The influence of pollution on the short wave albedo of clouds, *J. Atmos. Sci.*, *34*, 1149–1152, 1977.

Tzivion, S., G. Feingold, and Z. Levin, An efficient numerical solution to the stochastic collection equation, *J. Atmos. Sci.*, *44*, 3139–3149, 1987.

Tzivion, S., G. Feingold, and Z. Levin, The evolution of raindrop spectra, II, Collisional collection/breakup and evaporation in a rainshaft, *J. Atmos. Sci.*, *46*, 3312–3327, 1989.

Warren, S. G., C. J. Hahn, J. London, R. M. Chervine, and R. L. Jenne, Global distribution of total cloud cover and cloud type amounts over ocean, *NCAR Tech. Note*, *NCAR/TN-317+STR*, 42, 1986.

W. R. Cotton, S. M. Kreidenweis, and B. Stevens, Colorado State University, Department of Atmospheric Science, Fort Collins, CO 80523.

G. Feingold, CIRA/NOAA, 325 Broadway, Boulder, CO 80303.

(Received December 14, 1995; revised May 7, 1996; accepted May 7, 1996.)